

Automated cycle-slip correction of dual-frequency kinematic GPS data

Sunil B. Bisnath

Doctoral student
Department of Geodesy and Geomatics Engineering
University of New Brunswick
506-453-5088
s.bisnath@unb.ca

Richard B. Langley

Professor
Department of Geodesy and Geomatics Engineering
University of New Brunswick
506-453-5142
lang@unb.ca

Abstract

In order to attain high precision positioning and navigation results with GPS, cycle slips must be correctly repaired at the data preprocessing stage. Over the past decade a number of methods have been developed to detect and repair cycle slips. These methods invariably require user intervention for problematic cycle slips in portions of data, tuning of input parameters to data, or introduction of additional carrier-phase ambiguity-resolution parameters in the main data processing where preprocessing cycle-slip determination has failed. A method has been developed from various existing techniques, that provides fully automatic cycle-slip correction at the data preprocessing stage. Results indicate that single-cycle slips can be reliably detected for receivers in varied environments, and that these slips can be repaired correctly.

Introduction

The detection and correction of cycle slips is needed if accurate positioning is to be carried out. This task can be quite labour intensive if semi-automated techniques are used, or can produce erroneous results if inappropriate automated techniques are implemented. Slip detection and repair still represents a challenge to carrier phase data processing even after years of research, early on in which it was predicted [Westrop *et al.*, 1989] that cycle slips would in all likelihood not pose a problem in the future due to receiver advances.

This paper addresses the development of a cycle-slip detection and correction technique designed to detect and correct cycle slips in dual-frequency carrier phase data, in a fully automatic manner, utilising carrier phase and pseudorange measurements in a post-processing environment. The prime objective of the work is to correctly detect and repair *all* cycle slips in the data preprocessing stage, with straightforward algorithms not dependent on the quality of the input data.

Briefly, a cycle slip is a sudden integer number of cycles jump in the carrier phase observable, caused by the loss of lock of the receiver phase lock loops [Leick, 1995]. The loss may be due to internal receiver tracking problems or an interruption in the ability of the antenna to receive the satellite signals [Seeber, 1993]. A loss of lock may be shorter than the time interval between two adjacent data collection epochs or as long as the time interval between many epochs, in which case the term data gap may be in

order. The process of cycle-slip correction involves detecting the slip, estimating the exact number of L1 and L2 frequency cycles that comprise the slip, and actually correcting the phase measurements by these integer estimates.

For the most part, techniques used in the detection and determination of cycle slips have not changed drastically since the first methods were devised in the early 1980s. The focus has always been on attempting to develop a reliable, somewhat automatic detection and repair procedure. All methods have the common premise that to detect a slip at least one smooth (*i.e.*, low noise) quantity derived from the observations must be tested in some manner for discontinuities that may represent cycle slips [Hofmann-Wellenhof *et al.*, 1997].

The derived quantities usually consist of linear combinations of the undifferenced or double-differenced L1 and L2 carrier-phase and possibly pseudorange observations. Once the time series for the derived quantities have been produced, the cycle-slip detection process (that is, the detection of discontinuities in the time series) can be initiated. Detection methods include the use of time differencing, low degree polynomial fitting, and Kalman filtering (see, *e.g.*, Hofmann-Wellenhof *et al.*, [1997]; Seeber [1993]). After cycle slips have been detected, the actual number of L1 and L2 cycles that comprise each slip must be determined and then the data corrected. The latter is a simple enough task, but the determination can require additional information. This

complementary information usually comes in the form of an additional linear combination, which is used together with the detection combination to determine the cycle slip in terms of actual L1 and L2 cycles. If viable integer combinations cannot be determined, then additional carrier phase ambiguity resolution parameters can be introduced in the main data processing (*e.g.*, Kleusberg *et al.* [1993]; Seeber [1993]).

An automatic cycle-slip correction technique

The technique presented here represents an evolution, from static to kinematic and from semi-automatic to fully automatic data handling in the University of New Brunswick's DIPOP (Differential POSitioning Program) preprocessors [Kleusberg *et al.*, 1993]. After outlier detection and time tag correction, two satellite-receiver, geometry-free linear combinations are formed with the dual-frequency carrier phase and pseudorange measurements, for each baseline double-difference satellite pair.

Detection observables

The combinations chosen are the geometry-free phase and the widelane phase minus narrowlane pseudorange. Both of these combinations have been utilised for cycle-slip detection by Blewitt [1990] for undifferenced static data, and Gao and Li [1999] for double-differenced short baseline static and kinematic data.

Geometry-free phase

The first observable is the geometry-free phase linear combination:

$$\begin{aligned} & \lambda_1 \nabla \Delta \phi_1 - \lambda_2 \nabla \Delta \phi_2 \\ & = (\nabla \Delta d_{\text{ion}2} - \nabla \Delta d_{\text{ion}1}) + (\lambda_1 \nabla \Delta N_1 - \lambda_2 \nabla \Delta N_2) \\ & + (\nabla \Delta m_1 - \nabla \Delta m_2) + (\nabla \Delta \epsilon_1 - \nabla \Delta \epsilon_2), \end{aligned} \quad (1)$$

where λ_i is the carrier wavelength; ϕ_i is the measured carrier phase (in cycles); N_i is the number of cycles by which the initial phases are undetermined; $d_{\text{ion}i}$ is the delay due to the ionosphere; m_i and ϵ_i represent the effect of multipath and receiver noise on the carrier phases, respectively; and $\nabla \Delta$ is the double-difference operator.

This combination consists of inter-frequency double-difference ionosphere, L1 and L2 double-difference integer ambiguities, inter-frequency double-difference phase multipath, and inter-frequency double-difference receiver phase noise. A cycle slip on the next (post slip) epoch of this combination would result in the ambiguities term being replaced with

$$[\lambda_1 (\nabla \Delta N_1 + n_1) - \lambda_2 (\nabla \Delta N_2 + n_2)], \quad (2)$$

where n_1 and n_2 are the double-difference integer cycle-slips (in cycles) on the L1 and L2 frequencies, respectively.

Widelane phase minus narrowlane pseudorange

The second observable is the widelane phase minus narrowlane pseudorange linear combination (*e.g.*, Blewitt [1990]; Gao and Li [1999]):

$$\begin{aligned} & \lambda_4 (\nabla \Delta \phi_1 - \nabla \Delta \phi_2) - \lambda_5 \left(\frac{\nabla \Delta P_1}{\lambda_1} + \frac{\nabla \Delta P_2}{\lambda_2} \right) \\ & = \lambda_4 (\nabla \Delta N_1 - \nabla \Delta N_2) \\ & + \lambda_4 \left(\frac{\nabla \Delta m_1}{\lambda_1} - \frac{\nabla \Delta m_2}{\lambda_2} \right) - \lambda_5 \left(\frac{\nabla \Delta M_1}{\lambda_1} + \frac{\nabla \Delta M_2}{\lambda_2} \right) \\ & + \lambda_4 \left(\frac{\nabla \Delta \epsilon_1}{\lambda_1} - \frac{\nabla \Delta \epsilon_2}{\lambda_2} \right) - \lambda_5 \left(\frac{\nabla \Delta e_1}{\lambda_1} + \frac{\nabla \Delta e_2}{\lambda_2} \right) \end{aligned} \quad (3)$$

where P_i is the measured pseudorange (in distance units); M_i and e_i represent the effect of multipath and receiver noise on the pseudoranges, respectively;

$$\lambda_4 = (\lambda_1^{-1} - \lambda_2^{-1})^{-1} \approx 86.2 \text{ cm}, \quad (4)$$

usually referred to as the widelane wavelength;

$$\lambda_5 = (\lambda_1^{-1} + \lambda_2^{-1})^{-1} \approx 10.7 \text{ cm}, \quad (5)$$

usually referred to as the narrowlane wavelength; and the other terms are as stated in equation (1).

This combination consists of the widelane ambiguity, a residual multipath term, and a residual receiver noise term. Since the multipath and noise terms of the pseudorange measurements are much larger than those of the carrier phase measurement, the fluctuations in this combination are mainly due to pseudorange multipath and pseudorange measurement noise. The former of these error terms can cause quasi-sinusoidal variations of many metres. A cycle slip on the next (post slip) epoch of this combination would result in the ambiguities term being replaced with

$$\lambda_4 [(\nabla \Delta N_1 + n_1) - (\nabla \Delta N_2 + n_2)]. \quad (6)$$

The noise of this observable makes high resolution cycle-slip detection unlikely. However, Blewitt [1990] proposed a simple running average filter to make this observable more useful. This strategy is quite intuitive, since over time one would expect the residual multipath and noise terms to average down to near constant values.

Detection tests

Two different cycle-slip detection tests are performed on each time series of the created combinations. The geometry-free phase combination is first tested, since it has the lower noise. The first test investigates the variation of the normalised, between-epoch time difference of the geometry-free combination. Figure 1 illustrates this quantity. The principle used here is that a discontinuity in a time series is more pronounced in the time differences of that series, since time differencing is analogous to high-pass filtering [Hofmann-Wellenhof *et al.*, 1997]. From past experience with DIPOP [Kleusberg *et al.*, 1993], a set of four time differences are compared. The median time difference is differenced from the time difference value being tested. The absolute value of this difference leaves a very small component of the ionospheric, multipath and noise terms, and an estimate of the cycle slip, if any, on this combination. The resulting value is differenced from a slip tolerance parameter. In some software, (*e.g.*, Kleusberg *et al.* [1993]), this tolerance must be selected on a per data set basis. This human interaction has been removed in the new approach by computing the time difference of the smallest type of cycle slip that can consistently be observed with this combination (from equation (2)):

$$n_1 = 5, n_2 = 4 \Rightarrow |\lambda_1 n_1 - \lambda_2 n_2| \approx 2.5 \text{ cm.} \quad (7)$$

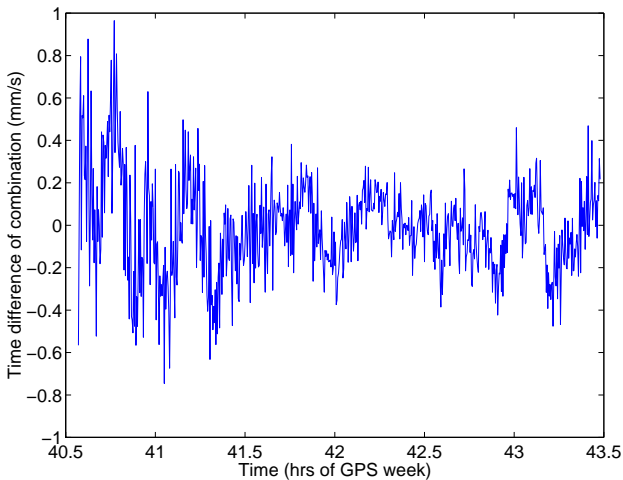


Figure 1: Time difference of geometry-free combination.

If a slip is detected, then the second test is carried out. The mean and standard deviation of the first four time differences are computed. If the difference under investigation lies outside $\pm 4\sigma$ of the mean (the 99.99% confidence interval) then a cycle slip is considered detected. The rationale for this second test stems from Blewitt [1990]. That is, the observation under investigation must be statistically similar to the

observations used in the test for a cycle slip not to have occurred. Conversely, the greater the dispersion in the observations used for the test, the greater the variability allowed in the particular observation under investigation.

For the widelane phase minus narrowlane pseudorange combination, a different approach is used due to the noise level of the combination. A testing scheme modelled after Blewitt's [1990] technique for undifferenced static data is used. The double-differenced measurements are filtered as stated and the unfiltered data points are compared with $\pm 4\sigma$ of the filtered average.

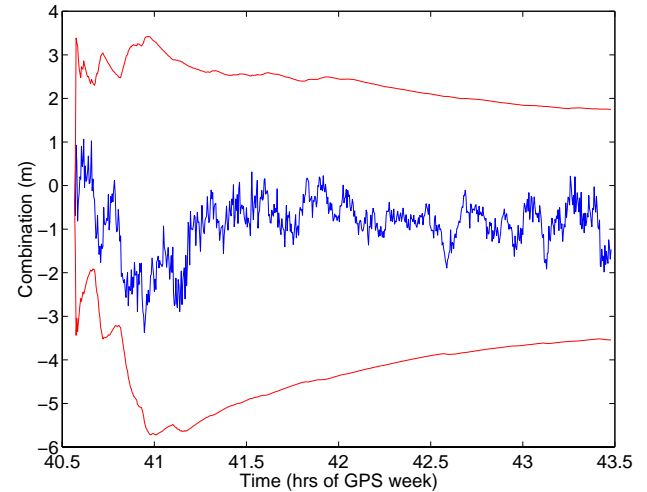


Figure 2: Variations in widelane phase minus narrowlane pseudorange combination with associated $\pm 4\sigma$ confidence intervals.

The meaning of this test is that any value outside the expected ambiguity estimate (the running average confidence interval) represents a possible cycle slip. If unfiltered data from subsequent epochs lie within one cycle of such a data point, then a slip is declared. An example of this testing is given in Figure 2.

Determination

To utilise the widelane phase minus narrowlane pseudorange combination, the forward and backward runs of the filter are combined to optimally smooth the time series.

The next step is the polynomial fitting. Chebyshev polynomial fitting was chosen for DIPOP [Kleusberg *et al.*, 1993] since it nearly completely minimises the maximum residuals in the fit, making it a very robust technique. A linear parametric least-squares fit of the polynomials to each linear data combination is then carried out in order to estimate the Chebyshev polynomial coefficients and more importantly the estimates of the cycle slips in each combination. The combination slip

estimates, the fit residuals, and the combination observations are then combined in a weighted parametric adjustment to estimate real-valued double-difference L1 and L2 cycle slips. These results are then rounded to obtain integer estimates.

Static data testing

In order to test the detection and determination strategy both static and kinematic data were processed. The former is presented here and the latter in the next section.

Static data testing was deemed appropriate, since it allows for a “truth solution” to be determined with a semi-automated technique, using less noisy phase combinations in the cycle-slip correction. The data set used consists of an approximately 200 km long baseline. The data contain a significant amount of multipath, which is representative of an extreme environment and therefore this data set provides a good test of robustness for the described slip correction technique.

The results using this strategy produced the same detected and repaired cycle slips as with the manual processing strategy. An example of a detected slip is shown in Figure 3. The slip can be observed at approximately 40.4 hours on this time difference of the geometry-free combination. The slip is equal to two double-difference cycles on L1 and two double-difference cycles on L2, and therefore is not detectable on the widelane phase minus the narrowlane pseudorange combination.

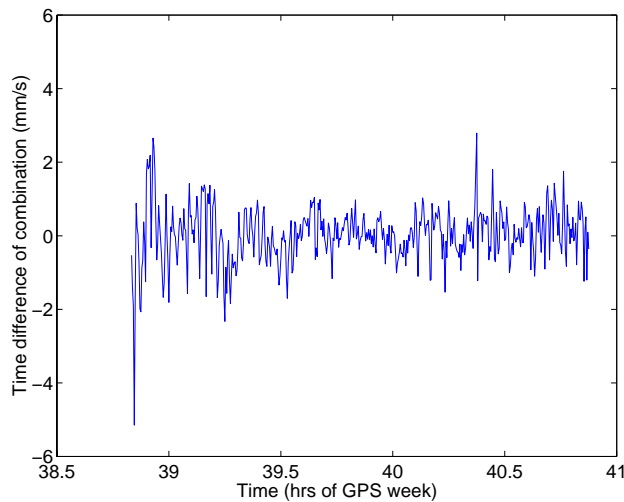


Figure 3: Detected cycle slip in static data using geometry-free phase combination.

Kinematic data testing

The kinematic tests involve a marine situation, in which the vessel data were collected at an average distance of 40 km from the reference receiver. This data set is

representative of typical measurement conditions. The “truth solution” was obtained via a complex Kalman filtering procedure with manual verification. The results using the presented strategy compare favourably with the Kalman filtering results in that both processing techniques produce the same results.

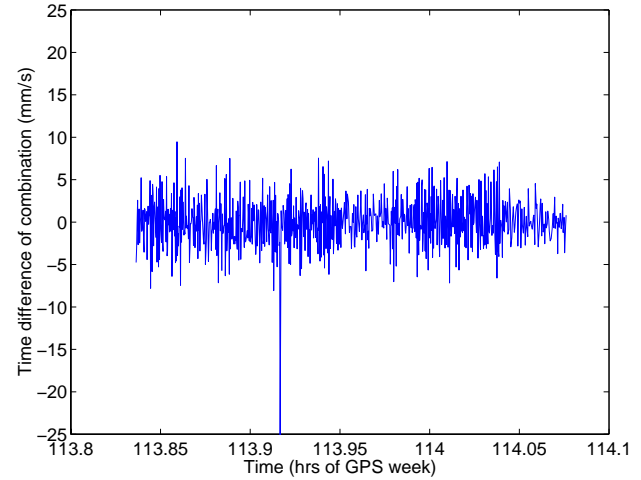


Figure 4: Detected cycle slip in kinematic data using geometry-free phase combination.

Certain cycle-slip pairs are difficult to detect with the described linear combinations, therefore various such slip pairs were injected into this kinematic data set to test the technique’s sensitivity. The results indicate that, with this data set, the most sensitive pairings can be detected and corrected with this technique. For example, the effect of the pairing $n_1 = 5, n_2 = 4$ (approximately a 2.5 cm jump in the geometry-free combination) can be clearly seen in Figure 4 at approximately 113.92 hours.

Conclusions and future work

A completely automatic cycle-slip detection, determination, and repair technique has been developed to preprocess dual-frequency, kinematic (and static) GPS data. The individual algorithms stem from research performed by various authors, and combined here in a novel procedure. The technique relies on the detection of cycle slips via two geometry-free linear combinations of the dual-frequency GPS measurements. The determination of detected slips is performed by integrating the two combinations in a Chebyshev polynomial, least-squares fitting scheme.

Results using extremely noisy static and typical kinematic data, with both actual and simulated cycle slips, indicate that the technique is correctly detecting and repairing cycle slips. Given that data sets vary significantly, more testing is required in order to further validate the

performance of the technique, particularly the robustness of the slip detection tests.

Acknowledgements

Financial support for this research was provided by the Natural Sciences and Engineering Research Council of Canada. Also acknowledged are colleagues Dr. Dong Hyun Kim for processing the kinematic data set from the Canadian Hydrographic Service and the Canadian Coast Guard, and Mr. Paul Collins for processing the static data set which includes data from the United States Continuously Operating Reference Stations (CORS) network.

References

- Blewitt, G. (1990). "An automatic editing algorithm for GPS data," *Geophysical Research Letters*, Vol. 17, No. 3, pp. 199-202.
- Gao, Y. and Z. Li, (1999). "Cycle slip detection and ambiguity resolution algorithms for dual-frequency GPS data processing," *Marine Geodesy*, Vol. 22, no. 4, pp. 169-181.
- Hofmann-Wellenhof, B., H. Lichtenegger, and J. Collins. (1997). *GPS Theory and Practice*. 4th Edition, Springer-Verlag, Wien, 389 pp.
- Kleusberg, A., Y. Georgiadou, F. van den Heuvel, and P. Heroux (1993). "GPS data preprocessing with DIPOP 3.0," internal technical memorandum, Department of Surveying Engineering (now Department of Geodesy and Geomatics Engineering), University of New Brunswick, Fredericton, 84 pp.
- Leick, A. (1995). *GPS Satellite Surveying*. 2nd Edition, John Wiley and Sons, Inc., New York, 560 pp.
- Seeber, G. (1993). *Satellite Geodesy*. Walter de Gruyter and Co., Berlin, 531 pp.
- Westrop, J, M.E. Napier, and V. Ashkenazi (1989). "Cycle slips on the move: detection and elimination." *Proceedings of the 2nd International Technical Meeting of the Satellite Division of the Institute of Navigation*, Colorado Springs, Colorado, U.S.A., 27-29 September, 1989, The Institute of Navigation, Alexandria, Virginia, U.S.A., pp. 31-34.